MOLECULAR AND CELLULAR BIOLOGY, June 1994, p. 3863–3875
0270-7306/94/$04.00+0

Vol. 14, No. 6

Fine-Resolution Mapping of Spontaneous and Double-Strand Break-Induced Gene Conversion Tracts in *Saccharomyces cerevisiae* Reveals Reversible Mitotic Conversion Polarity

DOUGLAS B. SWEETSER, HEATHER HOUGH, JENNIFER F. WHELDEN, MELISSA ARBUCKLE, AND JAC A. NICKOLOFF*

Department of Cancer Biology, Harvard University School of Public Health, Boston, Massachusetts 02115

Received 16 November 1993/Returned for modification 3 February 1994/Accepted 10 March 1994

Spontaneous and double-strand break (DSB)-induced gene conversion was examined in alleles of the *Saccharomyces cerevisiae ura3* gene containing nine phenotypically silent markers and an HO nuclease recognition site. Conversions of these alleles, carried on *ARS1/CEN4* plasmids, involved interactions with heteroalleles on chromosome V and were stimulated by DSBs created at HO sites. Crossovers that integrate plasmids into chromosomes were not detected since the resultant dicentric chromosomes would be lethal. Converted alleles in shuttle plasmids were easily transferred to *Escherichia coli* and analyzed for marker conversion, facilitating the characterization of more than 400 independent products from five crosses. This analysis revealed several new features of gene conversions. The average length of DSB-induced conversion tracts was 200 to 300 bp, although about 20% were very short (less than 53 bp). About 20% of spontaneous tracts also were also less than 53 bp, but spontaneous tracts were on average about 40% longer than DSB-induced tracts. Most tracts were continuous, but 3% had discontinuous conversion patterns, indicating that extensive heteroduplex DNA is formed during at least this fraction of events. Mismatches in heteroduplex DNA were repaired in both directions, and repair tracts as short as 44 bp were observed. Surprisingly, most DSB-induced gene conversion tracts were unidirectional and exhibited a reversible polarity that depended on the locations of DSBs and frameshift mutations in recipient and donor alleles.

Gene conversion is defined as the nonreciprocal transfer of two strands of information from one DNA duplex to a homologous duplex. Gene conversion has been widely studied in yeasts and other fungi and is evidenced during meiosis by 6:2 aberrant segregation patterns (43). Gene conversion also occurs in mitotic cells, e.g., yeast mating-type interconversion (21). Although gene conversion involves nonreciprocal information transfer, it is often associated with reciprocal exchange of markers flanking the converted region. Such exchanges are explained by models that invoke symmetric cross-strand structures (Holliday junctions [22]) that allow resolution of recombination intermediates in two senses, predicting flanking marker exchange in up to 50% of products (41).

An important feature of gene conversion is that close markers often coconvert. This feature indicates that gene conversion involves a region of DNA or tract, and many studies have shown that most conversion tracts are continuous (1, 3, 7, 8, 26, 61, 67). Conversion tract lengths have been measured for both meiotic and mitotic events. A controlled study comparing tract lengths for allelic *URA3* genes indicated that mitotic tracts were usually longer than 2 to 4 kbp, whereas meiotic tracts were usually shorter than 2 kbp (26). Average tract lengths were less than 500 bp for mitotic conversion between alleles in plasmids (3) or between nontandem duplications in a chromosome (1, 67). These shorter tracts probably reflect limitations imposed by the lengths of duplicated DNA at nonallelic loci. Also, conversion is diminished near borders of homology (2).

Double-strand breaks (DSBs) in regions of shared homology stimulate meiotic and mitotic gene conversion (27, 36, 38–40, 42, 45, 52, 53, 59; reviewed in reference 63). DSB-stimulated gene conversion is readily explained by the DSB repair model (62) and modifications thereof (58–60, 63, 66). In this model, DNA ends initiate recombination by invading homologous DNA elsewhere in the genome. A DSB may be enlarged into a gap before invasion. DNA synthesis, primed from the ends with the undamaged DNA as a template, repairs the break or gap and forms two Holliday junctions (22). Strand invasion and branch migration of Holliday junctions create heteroduplex DNA (hDNA) adjacent to the gap. In this model, gene conversion can result from gap repair and from mismatch repair of hDNA. Gap repair models explain continuous tracts by supposing that multiple markers exist within the gap and are supported by evidence that broken alleles are preferentially converted (36, 39, 42, 45).

Mating-type switching in the yeast *Saccharomyces cerevisiae* is a special case of DSB-induced intrachromosomal gene conversion of *MAT* that is stimulated by HO nuclease (21). *MAT* conversion apparently does not involve degradation of double-stranded regions to produce a gap (12). As first proposed by Strathern et al. (57) and later supported by White and Haber (66), *MAT* conversion involves a one-ended invasion of *HML* or *HMR* donor loci by a single 3′ end in the *MAT* Z region, displacing a donor strand that invades *MAT* sequences flanking *MAT* Y. *MAT* Y is subsequently cleaved by an endonuclease (as opposed to being degraded by an exonuclease), allowing repair synthesis. Sequences are converted only on the WXY side of the HO site, i.e., unidirectionally toward sequences *MAT* proximal to the DSB. The other end is apparently protected from the 5′-3′ exonuclease by association with the donor cassette (but not by homologous pairing), which may ensure selection of correct donor (66). In related models, single-stranded DNA is formed on both sides of a DSB (59, 60,

* Corresponding author. Mailing address: Department of Cancer Biology, Harvard School of Public Health, 665 Huntington Ave., Boston, MA 02115. Phone: (617) 432-1184. Fax: (617) 432-0107.

TABLE 1. Mutations in *ura3* created by linker insertion

Mutation[a]	Type	Location[b]	Insertion (bp)	Reference
Bgl205	*Bgl*II linker	*Pst*I	8	This study
X432	*Xho*I linker	*Nco*I	14	39
E432	*Eco*RI linker	*Nco*I	14	39
E764	*Eco*RI linker	X764	15	This study
HO432/OH432	HO site	E432	39	39
HO764/OH764	HO site	E764	37	This study
Xho1050	*Xho*I linker	*Nsi*I	6	This study

[a] Numbers in mutation names indicate positions within the 1.2-kbp *URA3* fragment (50). HO sites had 24 bp of homology to *MAT***a** (39); "OH" indicates site oriented with *MAT***a** Y sequences toward the 3′ end of *ura3*; "HO" indicates the opposite orientation.
[b] Natural or mutant restriction sites in *ura3*.

63), which is consistent with evidence for hDNA flanking converted *MAT* DNA (32, 46).

Alternative models explain gene conversion by invoking single-strand invasion followed by mismatch repair of hDNA (22, 33). These models explain continuous tracts by suggesting extensive or multiple hDNA regions and concerted repair toward one strand or long mismatch repair tracts. The majority of yeast meiotic conversion results from mismatch repair of hDNA (43). This conclusion was based on the observation that in mismatch repair-deficient *pms1* mutants, the frequency of 5:3 products increases (reflecting segregation of an unrepaired mismatch in hDNA) by the same amount that 6:2 conversions decrease.

It is clear that mitotic cells are able to effect gene conversion by gap repair, as demonstrated by transformation assays (42). However, it is not known whether spontaneous mitotic conversion is a consequence of gap repair, hDNA repair, or both processes. Sectored colonies arise at low frequencies among mitotic gene conversion products (e.g., references 48 and 49), providing evidence for hDNA intermediates in some events. However, it is not clear whether the low frequency of mitotic sectored colonies reflects frequent hDNA formation coupled with efficient mismatch repair, or frequent gap repair and limited involvement of hDNA.

Here we describe systems for mapping spontaneous and DSB-induced gene conversion tracts at a level of resolution of approximately 100 bp. This study demonstrates that conversion tracts are continuous in 97% of DSB-induced and spontaneous recombinant products, that tracts are often shorter than 53 bp, and that DSB-induced tracts usually extend unidirectionally from the DSB. This directionality was independent of HO site orientation but was reversible, depending on the positions of the DSB and frameshift mutations in the recipient and donor alleles, respectively. These results are discussed in relation to gene conversion mechanisms operating at *MAT* and at other loci.

MATERIALS AND METHODS

Plasmid DNA constructions. Plasmids were constructed by standard procedures (54) and prepared by using a modification of the procedure of Holmes and Quigley (23) as previously described (13). Site-directed mutagenesis was performed by unique site elimination mutagenesis (13) or by the method of Lewis and Thompson (29). Mutations were identified by restriction mapping and confirmed by dideoxy sequence analysis (United States Biochemical, Cleveland, Ohio). Plasmid pGalHOLys was constructed as follows. LYS2 was inserted into the *Hin*dIII site of pUC19 as a 4-kbp *Eco*RI-*Hin*dIII fragment (16) modified with *Hin*dIII linkers, creating pUCLys. The HO nuclease gene was excised from plasmid BlueHO (containing a PCR-generated fragment with *Hin*dIII sites flanking HO; courtesy of M. Hoekstra) as a 2.0-kbp *Xba*I-*Sal*I fragment and inserted into pUCLys, creating pHOLys. A 685-bp *Eco*RI-*Bam*HI *GAL1-10* promoter fragment was transferred from pBM150 (25) (courtesy of M. Johnston) to pUC19, producing pUCGal, and from pUCGal to pHOLys, creating pGalHOLys. *URA3* was manipulated as a 1.2-kbp *Hin*dIII fragment in a pUC19 derivative (pUCUra).

A *MAT***a**-*inc* allele was created by site-directed mutagenesis of a 3-kbp *Eco*RI-*Hin*dIII *MAT***a** fragment using a primer that creates a G→A transition at base Z2 (5′-TTCAGCTTTCCA CAACAGTAAA-3′). This mutation prevents mating-type interconversion (64) by blocking HO cleavage in vivo (38) but is not expected to alter mating or sporulation functions since it is outside *MAT***a** coding sequences (4). Plasmid pUraSupMata-inc was created with the *MAT***a**-*inc* fragment inserted between *URA3* and a 1.25-kbp *Eco*RI *SUP11* fragment.

TRP1/*ARS1*/*CEN4* (TAC) was excised as a 2.5-kbp *Eco*RI-*Bam*HI fragment from pSE271 (courtesy of P. Hieter), linked with *Bam*HI linkers, and subcloned into pHSS19 (37), creating pHSS19TAC. TAC was subsequently inserted into the *Bam*HI site of various pUCUra plasmids, creating the pUCUraTAC derivatives, all of which have identical orientations of *ura3* alleles and TAC sequences.

The identities of mutations used in this study are described in Tables 1 and 2. Phenotypically silent (Ura^+) restriction fragment length polymorphism (RFLP) mutations were created by site-directed mutagenesis or linker insertion. Silent mutations within *URA3* consisted of base substitutions at third positions of *URA3* codons. Frameshift mutations consisted of a linker insertion at *Nco*I (X432), a single base pair insertion

TABLE 2. Mutations in *ura3* created by primer-directed mutagenesis

Mutation[a]	Change(s)	Mispair(s)[b]	Mutagenic primer[c]
Ase20	C→A	G-A	TTCAATTCA**ATTAA**TCATTTTTT
Nsi304	C→T	G-T	TAATATC**ATGCAT**GAAAAGCAAAC
Pml409	T→C	A-C	CAAGATATC**CACGTG**TGTTTTTAG
Stu463	A→C	T-C	CCGCTAA**AGGCCT**TATCCGCCA
Bgl565	A→C	T-C	CT**GCCCATTCGGC**TATTCTGTAT
Ase667	C→T, T→A, G→A	G-T, A-A, C-A	GCTAAC**ATTAATAG**ACCTCTAGGTT
X764	TATC→CTAGA	4/5 bubble	CAAAGATTTTGT**CTAGA**GGCTTTATTGC
Nsi859	G→A	C-A	GACCCA**ATGCAT**CTCCCTTGTC

[a] All mutations are phenotypically Ura^+ except X764, which is a one-base frameshift that creates an in-frame TAG stop codon and an *Xba*I site.
[b] Wild-type base (in noncoding strand) is given first; mutant base (in coding strand) is given second.
[c] Mutant bases are underlined; newly created restriction sites are in boldface. The Ase667 mutation consists of three point mutations that create an *Ase*I site (AATAAT) and destroy a natural *Stu*I site at position 664 (AGGCCT converted to AGACCT).

TABLE 3. Yeast strains used

Strain[a]	Relevant genotype
YPH250	*MAT***a** *lys2-Δ1 ura3-52*
DY3017	*MAT***a** *lys2-Δ1:LYS2-GALHO ura3-52*
DY3023	*MAT***a**-*inc lys2-Δ1:LYS2-GALHO ura3-52*
DY3025	*MAT***a**-*inc lys2-Δ1:LYS2-GALHO URA3*
DY3026	*MAT***a**-*inc lys2-Δ1:LYS2-GALHO ura3*-X764
DY3028	*MAT***a**-*inc lys2-Δ1:LYS2-GALHO ura3*-X432
DY3029	*MAT***a**-*inc lys2-Δ1 ura3*-X764

[a] All strains have *ade2-101*, *his3-200*, *leu2-Δ1*, and *trp1-Δ1* markers.

(X764), and insertions of oligonucleotides containing 24-bp HO sites (HO432, OH432, HO764, and OH764 [39]). HO sites were oriented by DNA sequence analysis or by pairs of PCR amplifications using an HO-specific primer and *URA3*-specific primers. All frameshift mutations yielded Ura$^-$ phenotypes.

Yeast strains. All strains (Table 3) were derived from YPH250 (56) (a gift from M. Hoekstra). Yeast cells were transformed as described previously (24). Yeast DNA was prepared by a polyethylene glycol precipitation procedure (19). Chromosomal structures were confirmed by Southern hybridization analysis as described previously (39). DNA probes were labeled with [α-^{32}P]dCTP by random primer extension (17). DY3017 was created by integrative transformation (55) of YPH250 with *Xho*I-digested pGalHOLys. DY3023 is a *MAT***a**-*inc* derivative of DY3017 created by two-step replacement (55) of *MAT***a** by using pUraSupMata-inc cleaved with *Bgl*II, producing a white (*SUP11*-suppressed *ade2-101*), Ura$^+$ transformant that yielded red, Ura$^-$ recombinants when grown nonselectively (because of deletion of *SUP11* and *URA3*). DY3023 fails to switch mating type when *GALHO* is induced, confirming the *MAT***a**-*inc* phenotype (36). DY3025 was produced from DY3023 by direct transplacement with *URA3* (51). *ura3* alleles in DY3026 and DY3028 were produced by two-step replacements using a *SUP11*-red/white screen as described above and by selecting for resistance to 5-fluoro-orotic acid (6), respectively. DY3029 was produced from DY3026 by selection of Lys2$^-$, α-aminoadipate-resistant cells (11) that lost *LYS2* and *GALHO* by excisive recombination. Yeast strains harboring plasmid recombination substrates are named "strain:*ura3* allele." For example, DY3026 transformed with a TAC vector carrying *ura3* with nine RFLP markers and an HO site at position 432 is named DY3026:HO432.

Isolation and analysis of recombinant products. All recombinant products resulted from independent events. Independence was ensured since products were derived from independent Ura$^-$ colonies of parent strains. Recombinant products were isolated as papillae on uracil omission medium as described previously (38), with the following modifications. Parent cells were seeded to tryptophan omission plates to maintain TAC plasmids and grown for 2 days. Independent colonies were spread as 1-cm^2 patches on YP-glycerol plates and grown for 24 h (which reduces intracellular glucose and relieves repression of the *GAL1-10* promoter) before being replicated to YPD or YP-galactose plates. After 24 h, patches were replicated to uracil omission plates, and Ura$^+$ papillae were picked after 2 to 4 days. Ura$^+$ recombinants that convert plasmid-borne *ura3* alleles have unstable Ura$^+$ phenotypes upon nonselective growth as a result of spontaneous plasmid loss. These were identified among spontaneous Ura$^+$ recombinants by 24 h of nonselective growth on YPD medium, followed by plating of approximately 100 cells on nonselective medium and replica plating of the resulting colonies to medium missing uracil. Ura$^+$ stability tests were not performed

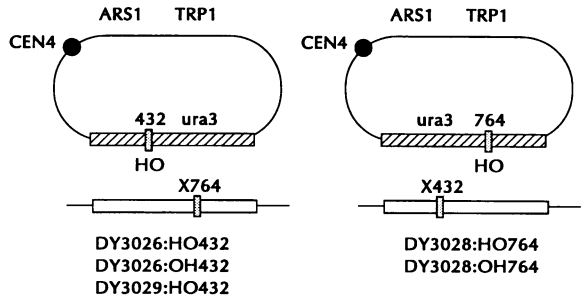

FIG. 1. Recombination substrates. Structures are shown for five crosses listed below. Duplicated 1.2-kbp fragments carrying *ura3* are shown by boxes. Alleles were inactivated by insertion mutations (shaded bars). Plasmid alleles have HO sites in two orientations flanked by nine silent RFLP mutations (hatching). Identities of mutations are given in Tables 1 and 2. All strains have *GALHO* and were used to isolate DSB-induced products, except DY3029:HO432, which was used to isolate spontaneous products.

for HO-induced products since HO-induced DSBs were expected to stimulate conversion of plasmid-borne alleles almost exclusively (39). Plasmid DNAs were transferred from Ura$^+$ recombinants to *Escherichia coli* HB101 or DH5α by electrotransformation of total yeast DNA. A single bacterial transformant from each Ura$^+$ recombinant was chosen for restriction analysis of silent RFLP markers. Control experiments, performed with two independent Ura$^+$ recombinants of DY3026:HO432, yielded four plasmids with identical RFLP patterns in each case, indicating that recombinants are clonal. Recombination frequencies were measured as described previously (39).

RESULTS

Strategy for fine-resolution mapping of gene conversion tracts. We constructed five strains containing *ura3* heteroalleles that allow mapping of gene conversion tracts at an approximately 100-bp level of resolution as a result of the presence of nine phenotypically silent, heteroallelic RFLP mutations (Fig. 1). A control *ARS1/CEN4* plasmid carrying a *URA3* allele with these nine RFLPs conferred Ura prototrophy, confirming the phenotypic silence of all nine RFLPs. Alleles containing the nine RFLPs in a low-copy-number plasmid were inactivated by HO site insertions. *ura3* heteroalleles, present at the normal chromosome V locus, were inactivated by insertion mutations but otherwise had wild-type sequences. Allele pairs were therefore heteroallelic at 11 positions. Strains carried *MAT***a**-*inc* mutations to prevent HO cleavage of *MAT* and subsequent mating-type interconversion and diploidization (31, 38). The HO nuclease recognition sequences in *HML* and *HMR* were not altered, as these are normally resistant to cleavage (21). Because glucose represses the *GAL1* promoter, cells were first grown in glycerol medium to reduce intracellular glucose and then transferred to galactose medium to induce HO nuclease. HO nuclease cleaves HO sites in plasmid *ura3* alleles, enhancing conversion of broken alleles more than 100-fold (38, 39). Without a functional HO nuclease, Ura$^+$ recombinants arise spontaneously at low frequencies (about 3×10^{-6}) by conversion of either plasmid or chromosomal alleles.

Functional Ura$^+$ recombinants may be produced by reciprocal (crossover) and nonreciprocal (gene conversion) exchange. However, crossovers integrate plasmids into the chromosomal *ura3* gene and produce lethal dicentric chromosomes. Therefore, this study focused on Ura$^+$ recombinants resulting from conversion of *ura3*

TABLE 4. RFLP mapping strategy

Digestion(s)[a]	Constant fragment(s) (bp)[b]	RFLP(s) present[c]	Variable fragment(s) (bp)[d]
*Ase*I	1235, 1216, 124, 59	**Ase20 + Ase667**	**3146, 647, 629**
		Ase20	3146, 1276
		Ase667	3793, 629
		Both absent	4422
*Bgl*II-*Xho*I	897	**Bgl205 + Xho1050**	**3621, 1693, 845**
		Bgl205	4466, 1693
		Xho1050	3621, 2538
		Both absent	6159
*Bgl*I	1118	**Bgl565**	**3970, 1968**
		Absent	5938
*Pml*I	None	**Pml409**	**3588, 3468**
		Absent	7056
*Stu*I	1007, 307	Stu463 + Stu664	3980, 1561, 201
		Stu463	**4181, 1561**
		Stu664	3980, 1762
		Both absent	5742
*Nsi*I-*Bam*HI	3200	Nsi304 + Nsi859 + Nsi1050	2776, 555, 334, 191
		Nsi304 + Nsi859	**2967, 555, 334**
		Nsi304 + Nsi1050	2776, 746, 334
		Nsi304	3522, 334
		Nsi859 + Nsi1050	2776, 889, 191
		Nsi859	2967, 889
		Nsi1050	2776, 1080
		All absent	3856

[a] Six restriction enzyme digests used to map nine RFLPs.
[b] Fragments of constant size (independent of RFLP status).
[c] For each digestion, two to eight RFLP arrangements are possible. Parental (unconverted) patterns are shown in boldface.
[d] Variable fragments for each RFLP arrangement.

alleles without associated integration. Conversions of plasmid *ura3* alleles to Ura$^+$ involved HO site loss since HO site insertions inactivate these alleles. However, since RFLP markers are phenotypically silent, RFLPs may be lost or retained. The nine RFLP markers were mapped in plasmids rescued from Ura$^+$ recombinants by using six restriction digestions (Table 4). Representative mapping data are shown in Fig. 2. RFLP loss by gene conversion restores wild-type sequences. RFLP loss by other mechanisms (i.e., mutagenesis) would yield the same results as loss by conversion for six RFLPs. However, three RFLPs occupy wild-type sites (Bgl205, Ase667, and Xho1050), and at these sites, correlations of RFLP loss with gain of wild-type sites indicate loss due to conversion. Loss of Ase667 always correlated with gain of a *Stu*I site at position 664 (*Ase*I and *Stu*I digests in Fig. 2, lane 1). Similarly, loss of Xho1050 always correlated with gain of an *Nsi*I site at position 1050. These results indicate that RFLP loss (for both linker insertions and substitution mutations) usually occurs by faithful conversion. Seven analyses were performed: (i) comparisons of spontaneous and DSB-induced recombination frequencies, (ii) allele conversion preferences, (iii) frequency of coconversion as a function of distance, (iv) average lengths of conversion tracts, (v) tract distributions, (vi) frequency and structures of discontinuous tracts, and (vii) mismatch repair in hDNA.

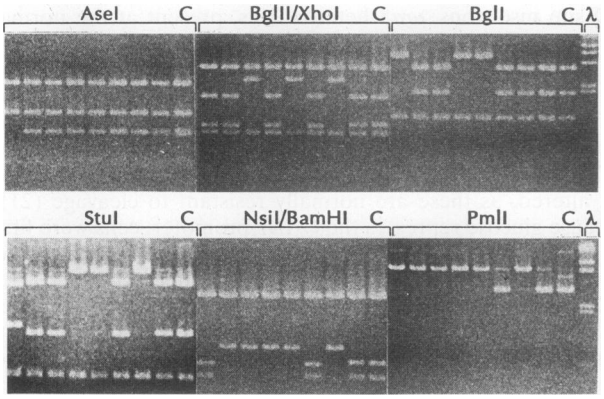

FIG. 2. Mapping RFLP markers. Shown are eight Ura$^+$ products from cross DY3029:HO432 plus nonconverted control DNA (C) digested with each of six sets of enzymes. Fragment identities can be determined from Table 4. Incomplete digestions with *Pml*I, evident in lanes 6, 8, and C, do not interfere with interpretations. Size markers are λ digested with *Hin*dIII.

Reversion of inactivating frameshift mutations. Control experiments were performed to measure the reversion frequency of inactivating mutations in chromosomal and plasmid *ura3* alleles. Plasmids with HO sites at *ura3* positions 432 and 764 were introduced into strains containing *ura3*-X432 and *ura3*-X764 alleles, respectively. The resulting strains were subjected to standard recombination assay culture and plating conditions (see Materials and Methods). Ura$^+$ revertants were not observed in any of four independent determinations with each strain (reversion rate, $<10^{-6}$).

Spontaneous and DSB-induced recombination frequencies. We measured induced and uninduced recombination frequencies for the crosses diagrammed in Fig. 1 to characterize the behavior of the different alleles (Table 5). HO-induced DSBs enhanced recombination by more than 400-fold in DY3026 crosses, similar to levels seen previously (39). When the positions of the HO site and chromosomal mutation were reversed (DY3028 crosses), HO also enhanced recombination, although to a lesser extent (about 80-fold). These differences may be a reflection of differences in plasmid copy numbers or chromosomal environment effects on the efficiency of HO nuclease cleavage (39). HO site orientation did not affect induced or uninduced recombination frequencies.

TABLE 5. Spontaneous and DSB-induced recombination frequencies

Cross[a]	Recombination frequency (10^{-6})[b]		Induction[c]
	Glucose grown	Galactose grown	
DY3026:OH432	1.9 ± 0.7	912 ± 112	480
DY3026:HO432	2.0 ± 0.3	830 ± 375	415
DY3028:OH764	0.9 ± 0.4	56 ± 12	62
DY3028:HO764	0.4 ± 0.2	45 ± 17	113
DY3029:HO432	0.6 ± 0.2	0.8 ± 0.2	

[a] Crosses are diagrammed in Fig. 1. Both DY3026 and DY3028 carry *GALHO* integrated at *LYS2*; DY3029 lacks a functional HO nuclease gene. HO sites are located and oriented in plasmid *ura3* alleles as described in Table 1.

[b] Average recombination frequencies ± standard deviations for four determinations are given for cultures grown in medium with glucose (uninduced) or galactose (HO induced).

[c] Calculated as the ratio of induced to uninduced frequencies.

Because we were interested in comparing spontaneous and DSB-induced gene conversion events, we were concerned that growth in medium with glycerol, which relieves repression of the *GAL1-10* promoter, might lead to low-level expression of HO and confound the analysis of spontaneous recombinants. We explored this possibility by comparing recombination frequencies for crosses DY3026:HO432 and DY3028:HO764 after growth for 2 days in glycerol or glucose medium. Ura$^+$ recombinants were formed almost 12-fold more frequently in DY3026:HO432 when repression was relieved than under repressing conditions, indicating that growth in glycerol medium leads to low-level *GALHO* expression. We therefore generated spontaneous products with DY3029, which is isogenic with DY3026 except that it lacks a functional HO nuclease gene and is *lys2-Δ1*. DY3029:HO432 grown in either glucose or galactose medium yields similar recombination frequencies (Table 5). DY3028:HO764 yielded similar Ura$^+$ frequencies under both growth conditions, which is consistent with the lower level of induced recombination in this strain (Table 5).

Allele conversion preferences. Spontaneous conversion events may convert plasmid-borne or chromosomal alleles. We tested 455 independent Ura$^+$ colonies from DY3029:HO432 and found that 87% had converted the chromosomal allele for glucose- or galactose-grown cells. For DSB-induced events, we expected broken (plasmid) alleles to be converted preferentially (39). Since HO induction increased recombination frequencies from 62- to about 450-fold (Table 5), we expected about 0.25 to 1.6% of induced DY3026 and DY3028 products, respectively, to have arisen spontaneously, with about 90% of these products converting chromosomal alleles. Surprisingly, about 3% of DY3026 products and 10% of DY3028 products isolated from induced cultures retained HO sites and all nine RFLPs (determined by restriction mapping and sequence analysis). These HO sites were cleavable (as assayed by recombination) when rescued plasmids were reintroduced into parent strains (data not shown). It is unlikely that the 6- to 12-fold excess of chromosomal convertants among products from induced cultures arose independently of DSBs at HO sites. These products may be produced by a hDNA-mediated mechanism by which DSBs in plasmid alleles induce chromosome conversions, as proposed earlier to account for the recombinogenic nature of DSBs in nonhomologous DNA (39, 52) and the low-frequency transfer of information from a broken allele to an unbroken allele (47). Alternatively, these unexpected products may result from multiple events or multiple resolutions of single events. These Ura$^+$ products were not analyzed further.

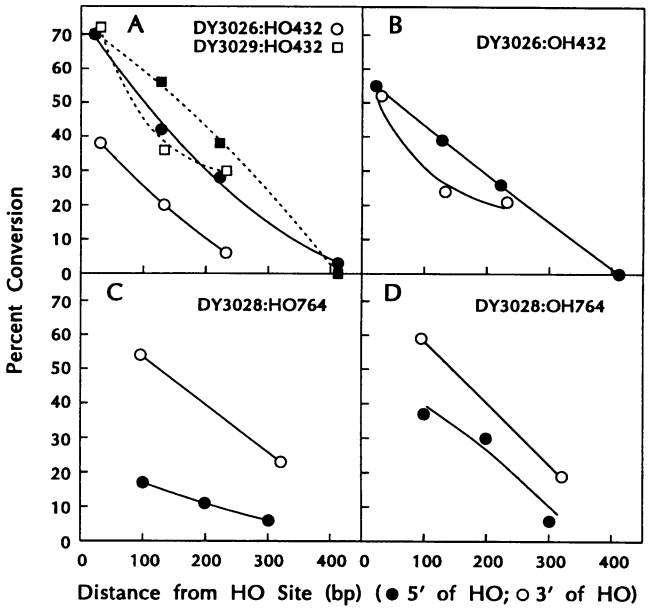

FIG. 3. Conversion frequency as a function of distance from HO sites. All data are for DSB-induced events, except data from the DY3029:HO432 cross (squares connected by dashed lines).

Percent coconversion of individual RFLPs as a function of distance from DSBs. Coconversion frequencies for RFLPs decreased as the distance from HO sites increased (Fig. 3). Interestingly, for DY3026 crosses, markers 5′ to HO (promoter proximal) were converted more frequently than equidistant markers 3′ to HO (promoter distal) (Fig. 3A and B), but this asymmetry was reversed in DY3028 crosses (Fig. 3C and D). Thus, reversing the position of plasmid DSBs and chromosomal mutations reverses conversion asymmetry (discussed further below). Also, four of seven markers (Nsi304, Stu463, Bgl565, and Ase667) were coconverted more frequently among spontaneous products than among DSB-induced products (P ranged from 0.05 to <0.0003; Fisher exact tests); Bgl205 also showed this trend, but the result was not statistically significant ($P = 0.08$).

Average conversion tract lengths. Crosses DY3026:HO432 and DY3029:HO432 provide a means to compare DSB-induced and spontaneous tract lengths among products of identical *ura3* alleles. Tract lengths were calculated as the mean of the longest and shortest possible lengths for each tract class. Spontaneous tracts averaged about 40% longer than DSB-induced tracts (202 versus 289 bp), which was manifested among spontaneous products as higher coconversion frequencies for individual RFLPs (discussed above). DSB-induced conversion tracts in DY3028 crosses (275 bp) were longer than in DY3026 crosses. However, the distances between the HO site and the two adjacent RFLPs in DY3028 crosses are greater than those in DY3026 crosses. Since a significant fraction of products converted only the HO site in both types of crosses (see below), the greater average tract length in DY3028 crosses is partly a reflection of the greater distances to markers adjacent to HO sites. HO site orientation did not significantly affect average tract length.

Distributions of continuous conversion tract classes: border effects, window effects, and DSB-induced unidirectional tract

TABLE 6. Tract parameters for continuous tracts in DY3026 and DY3029 crosses

Class[a]	Direction(s)[b]	Tract length (bp)			Tract windows (bp)[c]		
		Minimum	Maximum	Mean[d]	5′	3′	Net
1		0	54	27	23	31	54
2	5′	23	159	91	105	31	136
3	5′	128	258	193	99	31	130
4	5′	227	443	335	185	31	216
5	5′	412	463	438	20	31	51
6	3′	31	156	94	23	102	125
7	3′	133	258	196	23	102	125
8	3′	235	355	295	23	97	120
9	5′ and 3′	54	261	158	105	102	207
10	5′ and 3′	159	360	260	99	102	201
11	5′ and 3′	258	545	402	185	102	287
12	5′ and 3′	443	565	504	20	102	122
13	5′ and 3′	156	363	260	105	102	207
14	5′ and 3′	261	462	362	99	102	201
15	5′ and 3′	360	647	504	185	102	287
16	5′ and 3′	545	667	606	20	102	122
17	5′ and 3′	258	460	359	105	97	202
18	5′ and 3′	363	559	461	99	97	196
19	5′ and 3′	462	744	603	185	97	282
20	5′ and 3′	647	764	706	20	97	117

[a] Tract structures are shown in Fig. 4.
[b] Tract direction relative to HO site.
[c] Tract windows for 5′ and 3′ sides are distances between RFLPs on 5′ and 3′ sides of HO sites, respectively. Net = 5′ + 3′ windows.
[d] Calculated as half the sum of the minimum and maximum lengths.

asymmetries. Most spontaneous and DSB-induced recombination products had continuous conversion tracts. RFLPs distal to chromosomal mutations are not expected to be converted by gap repair but may be converted if included in hDNA, yielding products with discontinuous tracts (see below). Continuous tracts have several intrinsic parameters that may affect tract distributions, including length, direction relative to HO sites, and windows, defined as the distances separating converted and unconverted sites at tract ends (Tables 6 and 7). Tract distributions for the 20 continuous tracts for DY3026 and DY3029 crosses are shown in Fig. 4. Several conclusions can be drawn from these data. First, HO site orientation had little effect on the distribution of DSB-induced products from the DY3026 crosses. Second, about 20% of the products of the three crosses had tracts shorter than 54 bp, converting only the HO site, and tracts shorter than average (classes 1 to 3, 6, 7, and 9) were common. Tracts significantly longer than average (>350 bp; classes 5, 11, 12, and 14 to 20) were rare among DSB-induced products, accounting for only 9.4 and 20% of DY3026:OH432 and DY3026:HO432 products, respectively. In contrast, tracts of >350 bp accounted for 44.9% of spontaneous (DY3029:HO432) products. Third, the four classes that include a marker only 20 bp from the homology border (Ase20; classes 5, 12, 16, and 20) were extremely rare, with only one example among 171 spontaneous and DSB-induced products from the DY3029 cross and the two DY3026 crosses. Fourth, tract window size clearly affected tract class distributions. Despite the trend toward shorter tracts, long tracts were observed when windows were large. For example, tract classes 11, 15, and 19 (averaging 500 bp) have long windows (net window size averaging 290 bp) and were more frequent than classes 14 and 17, which have average lengths of 357 and 358 bp but windows about 90 bp shorter. Border effects also can be viewed in the context of window size. For example, the rare Ase20 border classes (5, 12, 16, and 20) have 20-bp 5′ windows. However, window size alone cannot account for the low

TABLE 7. Tract parameters for continuous tracts in DY3028 crosses[a]

Class	Direction(s)	Tract length (bp)			Tract windows (bp)		
		Minimum	Maximum	Mean	5′	3′	Net
1		0	192	96	97	95	192
2	5′	97	294	196	102	95	197
3	5′	199	396	298	102	95	197
4	5′	301	427	364	31	95	123
5	3′	95	485	290	97	191	288
6	3′	286	503	395	97	120	217
7	5′ and 3′	192	485	339	102	191	293
8	5′ and 3′	294	587	441	102	191	293
9	5′ and 3′	396	618	507	31	191	222
10	5′ and 3′	383	605	494	102	120	222
11	5′ and 3′	405	707	596	102	120	222
12	5′ and 3′	587	738	663	31	120	151

[a] Values are presented as described for Table 6.

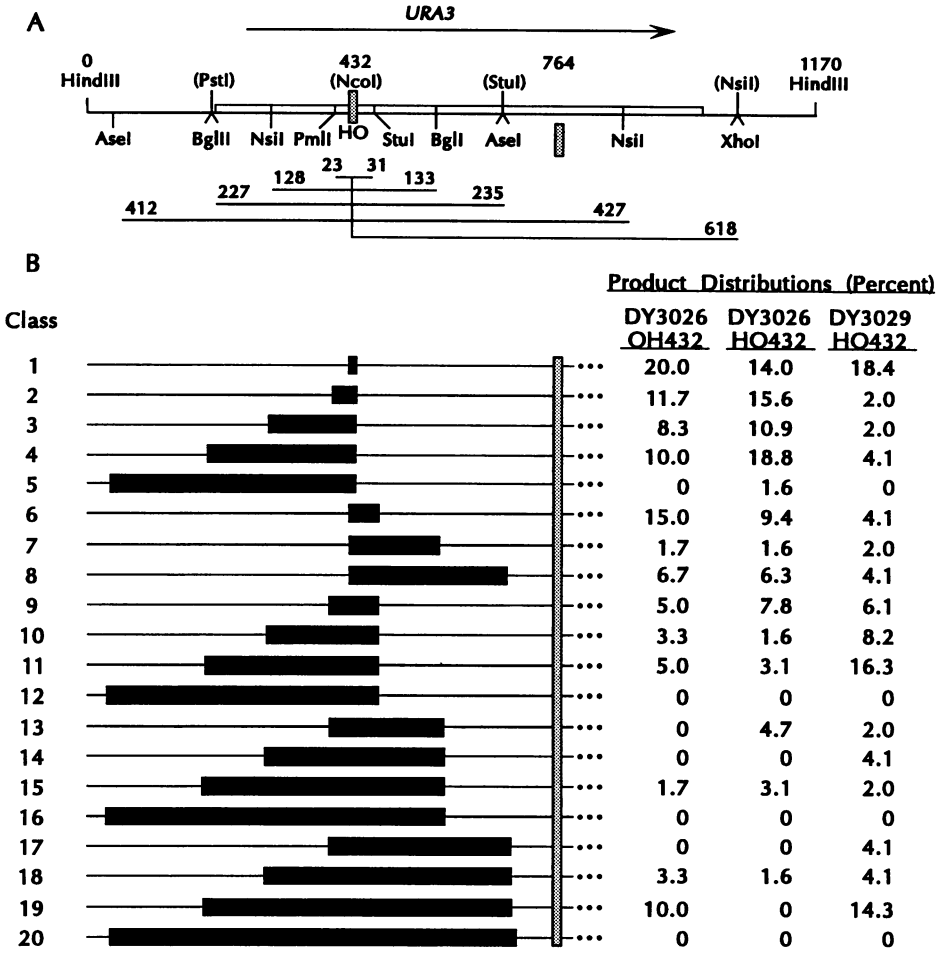

FIG. 4. Distributions of conversion tract classes for DY3026 and DY3029 crosses. (A) Map of *ura3* allele. Nine RFLP markers are shown below the line; wild-type sites are shown above the line. HO sites are present at position 432, a natural *Nco*I site. The chromosomal X764 frameshift mutation is shown by the shaded box below. Distances (in base pairs) are given between HO sites and RFLPs. (B) All 20 classes of gene conversion products with continuous tracts are shown. Black bars indicate converted markers. Continuous tracts that include HO sites cannot extend beyond X764. Percentages of each class are given for DSB-induced events (DY3026:OH432, 60 products; DY3026:HO432, 63 products) and spontaneous events (DY3029:HO432, 48 products).

frequencies of Ase20 border classes since other classes with similar windows occur much more frequently (see Discussion).

In the DY3028 crosses, the positions of the HO site and chromosomal *ura3* mutations are reversed, creating a different set of conversion tract classes. These classes and the distributions of products among them are shown in Fig. 5. Most of the conclusions from these results are similar to those from results for DY3026 crosses. Again, HO site orientation did not affect tract distributions, indicating that HO site orientation does not influence conversion mechanisms. The percentage of products that converted only the HO site (class 1) was higher for DY3028 crosses than for DY3026 crosses. However, this does not reflect a mechanistic difference but rather is a consequence of the closer spacing of markers adjacent to the HO432 site compared with the HO764 site. The closest marker to the homology border in the DY3028 crosses is Xho1050 (120 bp). Xho1050 was converted in 16 of 71 DY3028 products (23%), almost 40-fold more often than conversions of Ase20 in DY3026 crosses. Thus, if border effects occur at both 5′ and 3′ ends, effects are weak at markers 120 bp from a border.

As discussed above, coconversion of individual markers 5′ to DSBs was more frequent in DY3026 crosses than equidistant 3′ markers, and vice versa for DY3028 crosses. If we categorize the tract distribution data shown in Fig. 4 and 5 into unidirectional (5′ or 3′) and bidirectional tracts, it is clear that DSB-induced tracts are predominantly unidirectional (Fig. 6). Most spontaneous tracts include markers on both sides of the HO site. However, these tracts cannot be classified as bidirectional because it is not known where they initiate. Surprisingly, DSB-induced unidirectional tracts from DY3026 crosses extended primarily in a 5′ direction, whereas those from DY3028 crosses extended primarily in a 3′ direction. HO site orientation did not affect DSB-induced tract directionality. Thus, reversing the positions of DSBs in recipient alleles and mutations in donor alleles reverses tract directionality.

Three percent of spontaneous and DSB-induced conversion tracts are discontinuous. The results presented above included data from 302 independent recombinant products. Of these, 8 had discontinuous conversion tracts. An additional 137 products were isolated from DY3026 and DY3028 strains after noninducing growth conditions. Since we could not be certain whether these had arisen spontaneously or were induced by

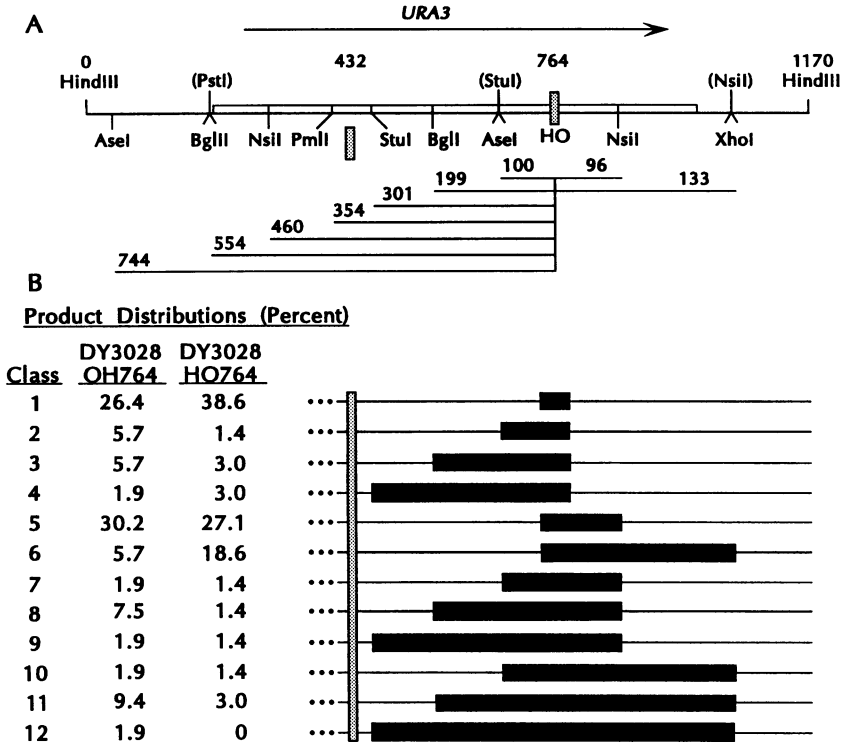

FIG. 5. Distributions of conversion tract classes for DY3028 crosses. (A) Map of the recipient *ura3* allele. Symbols are as in Fig. 4. (B) All 12 classes of gene conversion products with continuous tracts are shown. Continuous tracts that include HO sites cannot extend beyond X432. Percentages of each class are given for DSB-induced events in DY3028:OH764 (53 products) and DY3028:HO764 (70 products).

low-level HO expression, they were omitted from previous analyses. However, 5 of these 137 products (3.6%) had discontinuous tracts, and because products with discontinuous tracts occurred at similar frequencies among DSB-induced DY3026 and DY3028 products (3.1 and 1.6%, respectively) and spontaneous DY3029 products (4.0%), these five products with discontinuous tracts are included here to provide more complete data. Thus, we found a total of 13 products with discontinuous tracts among 439 isolates (3.0%); their structures are shown in Fig. 7.

Converted regions contiguous with HO sites may have been included in a gap or in hDNA. However, if gaps are involved, the maximum size of a gap is defined by the position of the first unconverted marker between converted regions. This allows the definition of minimum hDNA regions (assuming single hDNA tracts), which ranged up to 286 bp in length. It is not possible to determine the maximum extent of hDNA because mismatch correction or replicative segregation may lead to restoration of all markers distal to discontinuous regions of conversion. Mismatch repair can be inferred at markers flanked by two restored or two converted markers. When hDNA spans chromosomal mutations, we can infer a mismatch repair event with plasmid DNA as the template. Conversions of terminal markers in hDNA may occur either by mismatch repair (with chromosomal DNA as the repair template) or by replicative segregation of wild-type and mutant DNA.

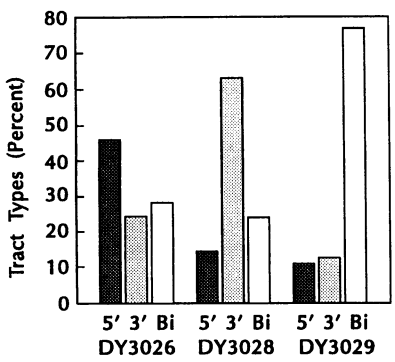

FIG. 6. Reversible DSB-induced mitotic conversion polarity. Data from Fig. 4 and 5 for crosses differing only by HO site orientation were pooled. Percentages of continuous tracts extending unidirectionally (5′ or 3′) and bidirectionally (Bi) from HO sites are plotted. Products converting only HO sites were excluded.

Twelve of these products had a single discontinuity and may have resulted from single mismatch repair events restoring one or two markers, or two independent repair events if two markers were restored. In products in which two markers may have been restored by a single repair tract (products 5 to 7 and 9), the minimum length of the repair tract would be 95 to 105 bp. One product is of particular interest, as it has two discontinuities (product 11 in Fig. 7). This is likely a product of an intermediate with hDNA spanning at least four markers, including three RFLPs and the chromosomal X432 mutation. A minimum of three independent mismatch repair tracts are required to generate this conversion pattern; two of them restored plasmid information (at X432 and Bgl565), and one converted Stu463 to chromosomal information. The terminal conversion at the Pml409 marker may have involved a fourth independent mismatch repair event, or as mentioned above, it may have been converted by replicative segregation. In any

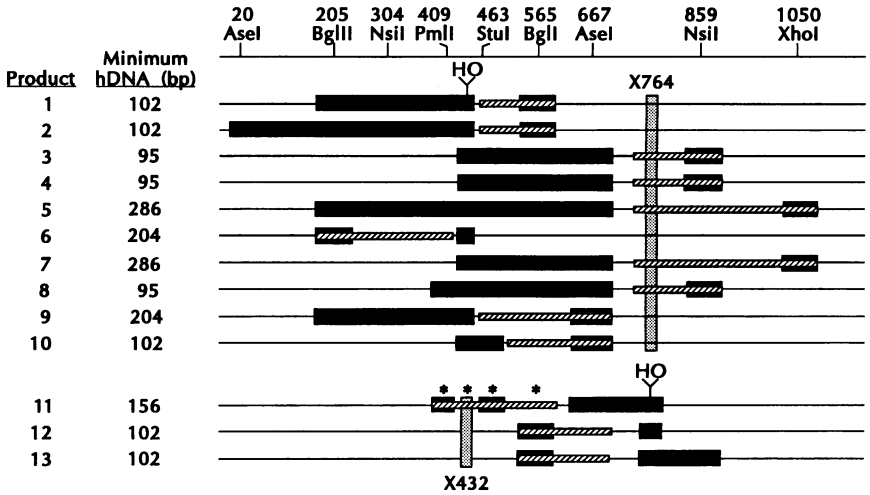

FIG. 7. Structures of discontinuous tracts. Symbols are as in Fig. 4. Minimum hDNA regions are hatched. Products 1 to 8 were isolated from DY3026:HO432 and DY3026:OH432. Products 9 and 10 arose spontaneously from DY3029:HO432. Products 11 to 13 were isolated from DY3028:HO764 and DY3028:OH764. Products 1 to 4, 11, and 12 were DSB induced. Products 5 to 8 and 13 arose following growth in medium with glycerol and transfer to medium with glucose. Asterisks mark positions of independent mismatch repair events in hDNA in product 11 (see text).

case, a minimum of three independent repair tracts for this product occurred in a region spanning only 133 bp, suggesting that mismatch repair tracts are as short as 44 bp in length.

The minimum length of conversion tracts among products with discontinuities averaged 523 bp, including continuous and discontinuous regions. This is longer than the average tract length among products with continuous tracts (200 to 300 bp). However, this difference, at least in part, reflects the limitation that continuous tracts terminate before chromosomal mutations.

Details about mismatch repair events in hDNA can be deduced from conversion patterns and predicted mismatches in minimum hDNA regions (Tables 1 and 2). Excluded from this analysis are mismatches formed by chromosomal X432 and X764 mutations since these must be repaired to wild-type sequences to produce the selected Ura$^+$ products. We have included mismatches at hDNA termini since it is likely that most mismatches are repaired before segregation (see Discussion). The results of this analysis, shown in Table 8, indicate that mismatch repair shows little bias toward particular bases among heteromismatches or toward particular strands for the A-A homomismatches. Three mismatch repair events involved loops formed by linker insertions at Bgl205 and Xho1050, and in all three cases, products had lost loops. Since these mismatches occurred at hDNA termini, conversions may have occurred by replicative segregation of unrepaired mismatches. These loops are very short palindromes (6 and 8 bp, respectively). In transformation assays, 8- and 12-bp palindromes rarely escape repair (1 to 15%). Nag et al. (35) showed that during meiosis, 26- to 36-bp palindromic loops often escape repair (30 to 80%).

TABLE 8. Mismatch repair events in hDNA

Mismatch[a]	Product[b]	No. of examples
T-C	G-C	6
T-C	T-A	5
C-A	T-A	4
C-A	C-G	6
G-T	A-T	3
G-T	G-C	2
A-A	T-A	2
A-A	A-T	2

[a] First bases listed for mismatches are wild-type and present in noncoding strands of chromosomal *ura3* alleles.

[b] Deduced products for repair events in minimum hDNA regions shown in Fig. 7.

DISCUSSION

We have developed a shuttle vector-based system that facilitates the rescue and analysis of large sets of independent gene conversion products. This system, combined with closely spaced silent RFLP markers, yields high sensitivity for detecting subtle gene conversion patterns and rare events. This study has confirmed the faithful information transfer of conversion events and has revealed new features of conversions, notably a reversible asymmetry for DSB-induced unidirectional conversions. These results provide new insights into several aspects of gene conversion mechanisms.

Lengths of spontaneous and DSB-induced conversion tracts. The amount of information transferred during gene conversion depends on the length of the gap or hDNA produced. Gap lengths depend on the competition between the rates of gap expansion and gap filling. hDNA lengths depend on the extent of strand exchange, which may depend on branch migration of Holliday junctions (33) or lengths of DNA involved in strand invasion. These factors suggest that coconversion frequencies should decrease as marker separation increases, a prediction borne out by this study and others (3, 39, 45). By placing markers very close to DSBs, we found that about 17% of conversion tracts were smaller than 54 bp, suggesting a slow rate of gap expansion, minimal hDNA, or hDNA repair favoring restoration of plasmid markers. Several studies have shown that HO-induced DSBs are repaired slowly both at *MAT* and other loci (12, 18, 39, 52, 53, 66), a result in

apparent conflict with very short conversion tracts, unless ends are protected from degradation (see below).

Tract length measurements are affected by a variety of factors. Mitotic recombination between heteroalleles is biased toward short conversion tracts since long continuous tracts do not produce selectable alleles. For spontaneous events, the average length of 289 bp observed here is shorter than that reported earlier for conversions between larger regions of homology (3), consistent with tract lengths being proportional to homology lengths (2). Also, long conversion tracts are associated with reciprocal exchange (1, 3), and single reciprocal exchanges are prohibited in our system. The markers used to measure tracts may influence tract lengths. In one study, multiple markers were shown to affect meiotic gene conversion and crossover frequencies (7), although no effects were seen in a second study (61). Multiple markers may reduce tract lengths by slowing the migration of Holliday junctions. Also, gene conversion tract lengths may vary for different genes, chromosomal loci, or allele arrangements, but these variables have not yet been systematically tested.

We found that spontaneous tracts were about 40% longer than DSB-induced tracts in identical crosses. This can be explained by a model in which spontaneous events are initiated at random sites within *ura3* (and perhaps outside *ura3* [39]). In our system, HO sites must be converted to produce Ura^+ plasmid alleles. If spontaneous events initiate randomly in *ura3*, few would be expected to occur very near HO sites and produce short tracts. This also may explain why most spontaneous tracts convert sites on both sides of the HO site, since tracts extending unidirectionally from the HO site may result only when initiated in the 54-bp interval between the two flanking markers (less than 5% of the total homology). Despite these apparent limitations, 18.4% of spontaneous products converted HO sites only. These products may arise when allele pairing produces hDNA across the HO site, producing a single-stranded loop that initiates a localized conversion event. Thus, although significantly different product spectra were obtained for DSB-induced and spontaneous events, we believe that this does not necessarily reflect mechanistic differences. Instead, it may reflect differences in positions of initiation sites.

Effects of homology borders and tract windows. The probability that a particular continuous tract class will be formed depends on several parameters intrinsic to each class. For example, long tracts will be rare if average tract lengths are short. Previously it was shown that spontaneous conversion of markers near homology borders occurs infrequently (2). In this study, we demonstrate similar border effects for DSB-induced events and provide evidence that border effects are not simply a consequence of narrow windows. Although tract window size clearly affected tract distributions, window size alone cannot explain the very rare conversion of the Ase20 border marker in DSB-induced DY3026 crosses (Fig. 4), since other tract classes with similar windows were much more frequent. For example, classes 1 and 5 have nearly identical windows, but class 1 was produced about 20 times more often than class 5. Also, the frequent classes 6, 7, and 8 have windows similar in size to those of the border class 12, but class 12 was never recovered. Although the Ase20 border classes are longer than average, other long tracts were not as rare (e.g., classes 15, 18, and 19). Thus, tract size alone cannot account for the rare Ase20 conversions. Ahn and Livingston (3) used a linker insertion near a homology border, leading them to propose that conversion near borders may be restricted because Holliday junctions are unable to migrate past a heterology unless sufficient base pairing can occur between the heterology and the border. In contrast, the Ase20 border marker in our study consists of a single base substitution and would therefore not be expected to interfere with Holliday junction migration. Another possibility is that Holliday junctions rarely migrate near homology borders regardless of the presence of heterologies.

As an alternative explanation for rare conversions of border markers, we suggest that gaps that include border markers may often extend past homology borders. This would preclude gap repair since homology is required on both sides of the gap for strand invasions. In this view, border effects are a reflection of gap repair boundaries. Although gaps that extend beyond homology borders may lead to recombination by single-strand annealing (30, 39, 52), this nonconservative mechanism cannot produce the conversion products observed here. Another interesting situation involving close markers occurs in the DY3028 crosses. Here, the chromosomal X432 mutation is a gap repair boundary since Ura^+ products are not recovered if gaps initiated at HO764 extend beyond position 432. The Stu463 marker occurs only 31 bp from this boundary, and it is rarely converted in DY3028 crosses (Fig. 5). This result is expected if gaps spanning HO764 and Stu463 often extend past position 432. Alternatively, if conversion is mediated by hDNA repair, we can explain the low frequency of Stu463 conversion by suggesting that Stu463 and X432 are usually corepaired. This is because repair of X432 hDNA produces Ura^+ products only when repaired toward plasmid (wild-type) sequences, and the corepair of Stu463 hDNA would not convert Stu463. However, corepair in hDNA does not readily account for the infrequent conversion of Ase20 in DY3026 crosses (discussed above). We cannot explain the low frequency of Stu463 conversions by the model suggesting that Holliday junction migration is inhibited by limited flanking homology (as with Ase20, discussed above) because Stu463 is flanked by large regions of homology.

Tract continuity. This study and others (reviewed in reference 43) have shown that most mitotic and meiotic gene conversion tracts are continuous. Several hypotheses have been advanced to explain tract continuity. In the gap repair model, tract continuity involves coconversion of multiple markers in a gap. hDNA repair models that invoke extensive hDNA or multiple hDNA regions explain continuity by requiring concerted repair events toward one strand or long mismatch repair tracts since unbiased hDNA repair would create patches of conversion. Detloff and Petes detected in yeast cells meiotic mismatch repair tracts that were 900 bp in length (14). In an in vitro study, mismatch repair tracts were shown to be less than 20 bp in length (34). However, only single mismatches were examined, so additional signals that might extend a repair tract were not present. If mitotic conversions usually involve hDNA repair, the high proportion of continuous tracts seen in this study and others (1, 3, 7, 8, 26, 61, 67) would suggest that repair tracts are usually long or concerted. We did find evidence for repair tracts as short as 44 bp (Fig. 7) and for repair of specific mispairs in both directions (Table 8), but these may represent rare cases. Alternatively, continuity of hDNA-mediated conversions may result from replication of hDNA before mismatch repair (10). We believe this is unlikely in view of the evidence for efficient mismatch repair systems (5, 28), low frequencies of postmeiotic segregation (reviewed in reference 43), and increased levels of marker segregation in hDNA during mitotic conversion of *MAT* in *pms1* mutants (46). Another possibility is that unbiased correction leads initially to patches of conversion, with patches removed by subsequent mismatch repair-induced recombination (9). In this view, the rare products that retain patches presumably avoided secondary repair-induced recombination events. Recent evidence arguing against this model for mitotic events

comes from crosses using *ura3* alleles similar to those described here in which DSB-induced conversions to Ura^+ were not possible by gap repair but were possible by an hDNA-mediated mechanism. In these crosses, all products had discontinuous tracts (65).

DSBs stimulate unidirectional mitotic conversions with reversible polarity: implications for *MAT* switching and meiotic polarity gradients. By measuring many gene conversion tracts at high resolution, we have uncovered a novel type of polarity for mitotic events stimulated by DSBs. Most DSB-induced conversion tracts extend unidirectionally from the DSB, with markers only 20 to 30 bp from the DSB remaining unconverted on one side of the break. Asymmetric conversions can be explained by several models. They may result from protection of one end of a DSB. However, if this is true, such protection is independent of the orientation of the HO site, since HO site orientation had no detectable effects in this or previous studies (36, 53). Alternatively, gaps may normally be extended in only one direction. In models invoking 3′ single-stranded tails (60, 66), such tails may be formed on only one side of the break. Clearly, gap filling involves the formation of hDNA at both ends of a gap when 3′ ends invade donor loci. hDNA may be limited on one side of the gap, or hDNA on one side may be repaired in favor of the invading strand, suppressing conversion of markers on this side. However, at *MAT***a**, mismatches in hDNA near DSBs were repaired in the opposite sense, i.e., against the invading strand (20), possibly because of biased mismatch repair or proofreading activity of DNA polymerase acting on invading 3′ ends. It was suggested that the repair in favor of *HML* was not due to proofreading because segregation increased in *pms1* strains (20). However, this conclusion assumes that Pms1 is not involved in proofreading. Conversion asymmetry may involve differential hDNA repair bias on either side of a DSB. DSBs stimulate asymmetric conversion of *MAT*, toward *MAT* Y sequences (21). *MAT* conversion may represent an adaptation of a general consequence of DSB-induced mitotic conversion that may be facilitated by accessory proteins. Alternatively, conversion asymmetries may be stronger for intrachromosomal conversions than for plasmid × chromosome conversions.

The observed reversible polarity may depend only on the position of the DSB or only on the position of mutations in donor loci. Although it is possible that some properties of the conversions examined in this study were affected by the presence of the nine heterozygous markers (such as tract lengths), it is difficult to imagine how markers located across the entire length of homology could cause a reversal of polarity. The observed effect may reflect the recovery of a subset of DSB-induced conversions that are not associated with reciprocal exchange. For example, if conversions of sites toward the greater length of homology are often associated with crossovers, these conversions would not be detected. Both the observed polarity and its reversibility can be explained by a model in which conversion of markers in the interval between DSBs and the position of the chromosomal frameshift mutations often involves coconversion of the chromosomal mutation. This would transfer a frameshift mutation to the plasmid and reduce the frequency of products with markers converted in this interval. Such coconversion might result from repair of gaps encompassing this interval or from hDNA repair bias as a result of corepair due to long mismatch repair tracts (discussed above).

Meiotic gene conversion frequencies vary across the length of genes (43), with markers at one end converting more frequently than markers at the other end. These polarity gradients may reflect the presence of preferred initiation sites for hDNA formation, as suggested for sites susceptible to DSBs at *ARG4* (40, 59, 60). Since most meiotic conversion involves hDNA repair, this model suggests that hDNA forms more often near initiation sites than at more distant sites. At *ARG4*, DSBs initiate bidirectional conversions (60). In contrast, meiotic polarity at *HIS4* is not a consequence of a gradient of hDNA formation across the gene but results instead from differential mismatch repair bias at different distances from the initiation site (15). Also, the *HIS4* initiation site stimulates unidirectional conversions, a finding that raised the question of whether the *HIS4* initiation site is susceptible to DSBs (44). However, our data clearly show that DSBs can stimulate unidirectional conversions. Polarity gradients have never been observed for mitotic conversions arising spontaneously or induced by radiation and chemical agents (43). This may be a consequence of a lack of preferred initiation sites for mitotic conversions. However, in view of the observation that the *HIS4* meiotic polarity gradient results from biased mismatch repair (15), the lack of polarity in mitotic recombination might reflect less frequent hDNA involvement and more gap repair. If mitotic recombination is frequently mediated by hDNA repair, then the lack of mitotic polarity may reflect different hDNA repair biases in mitosis and meiosis.

ACKNOWLEDGMENTS

We are grateful for helpful comments from Merl Hoekstra, F. Andrew Ray, Elizabeth Miller, Danielle Taghian, and the reviewers.

This research was supported by grant CA 55302 to J.A.N. from the National Institutes of Health.

REFERENCES

1. **Aguilera, A., and H. L. Klein.** 1989. Yeast intrachromosomal recombination: long gene conversion tracts are preferentially associated with reciprocal exchange and require the *RAD1* and *RAD3* gene products. Genetics **123:**683–694.
2. **Ahn, B.-Y., K. J. Dornfeld, T. J. Fagrelius, and D. M. Livingston.** 1988. Effect of limited homology on gene conversion in a *Saccharomyces cerevisiae* plasmid recombination system. Mol. Cell. Biol. **8:**2442–2448.
3. **Ahn, B.-Y., and D. M. Livingston.** 1986. Mitotic gene conversion lengths, coconversion patterns, and the incidence of reciprocal recombination in a *Saccharomyces cerevisiae* plasmid system. Mol. Cell. Biol. **6:**3685–3693.
4. **Astell, C., L. Ahlstrom-Jonasson, M. Smith, K. Tatchell, K. A. Nasmyth, and B. D. Hall.** 1981. The sequence of the DNAs coding for the mating-type loci of *Saccharomyces cerevisiae*. Cell **27:**15–23.
5. **Bishop, D. K., J. Andersen, and R. D. Kolodner.** 1989. Specificity of mismatch repair following transformation of *Saccharomyces cerevisiae* with heteroduplex plasmid DNA. Proc. Natl. Acad. Sci. USA **86:**3713–3717.
6. **Boeke, J. D., F. Lacroute, and G. R. Fink.** 1984. A positive selection for mutants lacking orotidine-5′-phosphate decarboxylase activity in yeast: 5-fluoro-orotic acid resistance. Mol. Gen. Genet. **197:**345–346.
7. **Borts, R. H., and J. E. Haber.** 1987. Meiotic recombination in yeast: alteration by multiple heterozygosities. Science **237:**1459–1465.
8. **Borts, R. H., and J. E. Haber.** 1989. Length and distribution of meiotic gene conversion tracts and crossovers in *Saccharomyces cerevisiae*. Genetics **123:**69–80.
9. **Borts, R. H., W. Y. Leung, W. Kramer, B. Kramer, M. Williamson, S. Fogel, and J. E. Haber.** 1990. Mismatch repair-induced meiotic recombination requires the pms1 gene product. Genetics **124:**573–584.
10. **Bruschi, C. V., and M. S. Esposito.** 1983. Enhancement of spontaneous mitotic recombination by the meiotic mutant *spo11-1* in *Saccharomyces cerevisiae*. Proc. Natl. Acad. Sci. USA **80:**7566–7570.
11. **Chattoo, B. B., F. Sherman, D. A. Atubalis, T. A. Fiellstedt, D. Mehnert, and M. Ogur.** 1979. Selection of lys2 mutants of the

yeast *Saccharomyces cerevisiae* by the utilization of α-aminoadipate. Genetics **93**:51–65.
12. **Connolly, B., C. I. White, and J. E. Haber.** 1988. Physical monitoring of mating type switching in *Saccharomyces cerevisiae*. Mol. Cell. Biol. **8**:2342–2349.
13. **Deng, W. P., and J. A. Nickoloff.** 1992. Site-directed mutagenesis of virtually any plasmid by eliminating a unique site. Anal. Biochem. **200**:81–88.
14. **Detloff, P., and T. D. Petes.** 1992. Measurements of excision repair tracts formed during meiotic recombination in *Saccharomyces cerevisiae*. Mol. Cell. Biol. **12**:1805–1814.
15. **Detloff, P., M. A. White, and T. D. Petes.** 1992. Analysis of a gene conversion gradient at the HIS4 locus in Saccharomyces cerevisiae. Genetics **132**:113–123.
16. **Eibel, H., and P. Philippsen.** 1983. Identification of the cloned *S. cerevisiae LYS2* gene by an integrative transformation approach. Mol. Gen. Genet. **191**:66–73.
17. **Feinberg, A. P., and B. Vogelstein.** 1983. A technique for radiolabeling DNA restriction endonuclease fragments to high specific activity. Anal. Biochem. **132**:6–13.
18. **Fishman-Lobell, J., N. Rudin, and J. E. Haber.** 1992. Two alternative pathways of double-strand break repair that are kinetically separable and independently modulated. Mol. Cell. Biol. **12**:1292–1303.
19. **Fujimura, H., and Y. Sakuma.** 1993. Simplified isolation of chromosomal and plasmid DNA from yeasts. BioTechniques **14**:538–539.
20. **Haber, J. E., B. L. Ray, J. M. Kolb, and C. I. White.** 1993. Rapid kinetics of mismatch repair of heteroduplex DNA that is formed during recombination in yeast. Proc. Natl. Acad. Sci. USA **90**: 3363–3367.
21. **Herskowitz, I., J. Rine, and J. N. Strathern.** 1992. Mating-type determination and mating-type interconversion in *Saccharomyces cerevisiae*, p. 583–656. *In* E. W. Jones, J. R. Pringle, and J. R. Broach, (ed.), The molecular and cellular biology of the yeast *Saccharomyces*, vol. 2. Cold Spring Harbor Laboratory Press, Cold Spring Harbor, N.Y.
22. **Holliday, R.** 1964. A mechanism for gene conversion in fungi. Genet. Res. (Cambridge) **5**:282–304.
23. **Holmes, D. S., and M. Quigley.** 1981. A rapid boiling method for the preparation of bacterial plasmids. Anal. Biochem. **114**:193–197.
24. **Ito, H., Y. Fukuda, K. Murata, and A. Kimura.** 1983. Transformation of intact yeast cells treated with alkali cations. J. Bacteriol. **153**:163–168.
25. **Johnston, M., and R. W. Davis.** 1984. Sequences that regulate the divergent *GAL1-GAL10* promoter in *Saccharomyces cerevisiae*. Mol. Cell. Biol. **4**:1440–1448.
26. **Judd, S. R., and T. D. Petes.** 1988. Physical lengths of meiotic and mitotic gene conversion tracts in *Saccharomyces cerevisiae*. Genetics **118**:401–410.
27. **Kolodkin, A. L., A. J. S. Klar, and F. W. Stahl.** 1986. Double-strand breaks can initiate meiotic recombination in *S. cerevisiae*. Cell **46**:733–740.
28. **Kramer, B., W. Kramer, M. S. Williamson, and S. Fogel.** 1989. Heteroduplex DNA correction in *Saccharomyces cerevisiae* is mismatch specific and requires functional *PMS* genes. Mol. Cell. Biol. **9**:4432–4440.
29. **Lewis, M. K., and D. V. Thompson.** 1990. Efficient site directed *in vitro* mutagenesis using ampicillin selection. Nucleic Acids Res. **18**:3439–3443.
30. **Lin, F.-L., K. Sperle, and N. Sternberg.** 1984. Model for homologous recombination during transfer of DNA into mouse L cells: role for DNA ends in the recombination process. Mol. Cell. Biol. **4**:1020–1034.
31. **Mascioli, D. W., and J. E. Haber.** 1980. A cis-dominant mutation within the *MAT***a** locus of *Saccharomyces cerevisiae* that prevents efficient homothallic mating type switching. Genetics **94**:341–360.
32. **McGill, C., B. Shafer, and J. Strathern.** 1989. Coconversion of flanking sequences with homothallic switching. Cell **57**:459–467.
33. **Meselson, M., and C. M. Radding.** 1975. A general model for genetic recombination. Proc. Natl. Acad. Sci. USA **72**:358–361.
34. **Muster-Nassal, C., and R. Kolodner.** 1986. Mismatch correction catalyzed by cell-free extracts of *Saccharomyces cerevisiae*. Proc. Natl. Acad. Sci. USA **83**:7618–7622.
35. **Nag, D. K., M. A. White, and T. D. Petes.** 1989. Palindromic sequences in heteroduplex DNA inhibit mismatch repair in yeast. Nature (London) **340**:318–320.
36. **Nickoloff, J. A., E. Y. C. Chen, and F. Heffron.** 1986. A 24-base-pair sequence from the MAT locus stimulates intergenic recombination in yeast. Proc. Natl. Acad. Sci. USA **83**:7831–7835.
37. **Nickoloff, J. A., and R. J. Reynolds.** 1991. Subcloning with new ampicillin and kanamycin resistant analogs of pUC19. BioTechniques **10**:469–472.
38. **Nickoloff, J. A., J. D. Singer, and F. Heffron.** 1990. In vivo analysis of the *Saccharomyces cerevisiae* HO nuclease recognition site by site-directed mutagenesis. Mol. Cell. Biol. **10**:1174–1179.
39. **Nickoloff, J. A., J. D. Singer, M. F. Hoekstra, and F. Heffron.** 1989. Double-strand breaks stimulate alternative mechanisms of recombination repair. J. Mol. Biol. **207**:527–541.
40. **Nicolas, A., D. Treco, N. P. Shultes, and J. W. Szostak.** 1989. An initiation site for meiotic gene conversion in the yeast *Saccharomyces cerevisiae*. Nature (London) **338**:35–39.
41. **Orr-Weaver, T. L., and J. W. Szostak.** 1985. Fungal recombination. Microbiol. Rev. **49**:33–58.
42. **Orr-Weaver, T. L., J. W. Szostak, and R. J. Rothstein.** 1981. Yeast transformation: a model system for the study of recombination. Proc. Natl. Acad. Sci. USA **78**:6354–6358.
43. **Petes, T. D., R. E. Malone, and L. S. Symington.** 1991. Recombination in yeast, p. 407–521. *In* J. R. Broach, E. W. Jones, and J. R. Pringle (ed.), The molecular and cellular biology of the yeast *Saccharomyces*: genome dynamics, protein synthesis, and energetics, vol. I. Cold Spring Harbor Laboratory Press, Cold Spring Harbor, N.Y.
44. **Porter, S. E., M. A. White, and T. D. Petes.** 1993. Genetic evidence that the meiotic recombination hotspot at the HIS4 locus of Saccharomyces cerevisiae does not represent a site for a symmetrically processed double-strand break. Genetics **134**:5–19.
45. **Ray, A., I. Siddiqi, A. L. Kolodkin, and F. W. Stahl.** 1988. Intrachromosomal gene conversion induced by a DNA double-strand break in *Saccharomyces cerevisiae*. J. Mol. Biol. **201**:247–260.
46. **Ray, B. L., C. I. White, and J. E. Haber.** 1991. Heteroduplex formation and mismatch repair of the "stuck" mutation during mating-type switching in *Saccharomyces cerevisiae*. Mol. Cell. Biol. **11**:5372–5380.
47. **Roitgrund, C., R. Steinlauf, and M. Kupiec.** 1993. Donation of information to the unbroken chromosome in double-strand break repair. Curr. Genet. **23**:414–422.
48. **Roman, H., and F. Fabre.** 1983. Gene conversion and associated reciprocal recombination are separable events in vegetative cells of Saccharomyces cerevisiae. Proc. Natl. Acad. Sci. USA **80**:6912–6916.
49. **Ronne, H., and R. Rothstein.** 1988. Mitotic sectored colonies: evidence of heteroduplex DNA formation during direct repeat recombination. Proc. Natl. Acad. Sci. USA **85**:2696–2700.
50. **Rose, M., P. Grisafi, and D. Botstein.** 1984. Structure and function of the yeast *URA3* gene: expression in *Escherichia coli*. Gene **29**:113–124.
51. **Rothstein, R. J.** 1983. One-step gene disruption in yeast. Methods Enzymol. **101**:202–211.
52. **Rudin, N., and J. E. Haber.** 1988. Efficient repair of HO-induced chromosomal breaks in *Saccharomyces cerevisiae* by recombination between flanking homologous sequences. Mol. Cell. Biol. **8**:3918–3928.
53. **Rudin, N., E. Sugarman, and J. E. Haber.** 1989. Genetic and physical analysis of double-strand break repair and recombination in *Saccharomyces cerevisiae*. Genetics **122**:519–534.
54. **Sambrook, J., E. F. Fritsch, and T. Maniatis.** 1989. Molecular cloning: a laboratory manual, 2nd ed. Cold Spring Harbor Laboratory Press, Cold Spring Harbor, N.Y.
55. **Scherer, S., and R. W. Davis.** 1979. Replacement of chromosome segments with altered DNA sequences constructed *in vitro*. Proc. Natl. Acad. Sci. USA **76**:4951–4955.
56. **Sikorski, R. S., and P. Hieter.** 1989. A system of shuttle vectors and yeast host strains designed for efficient manipulation of DNA in

Saccharomyces cerevisiae. Genetics **122:**19–27.

57. **Strathern, J. N., A. J. S. Klar, J. B. Hicks, J. A. Abraham, J. M. Ivy, K. A. Nasmyth, and C. McGill.** 1982. Homothallic switching of yeast mating type cassettes is initiated by a double-stranded cut in the *MAT* locus. Cell **31:**183–192.
58. **Sugawara, N., and J. E. Haber.** 1992. Characterization of double-strand break-induced recombination: homology requirements and single-stranded DNA formation. Mol. Cell. Biol. **12:**563–575.
59. **Sun, H., D. Treco, N. P. Schultes, and J. W. Szostak.** 1989. Double-strand breaks at an initiation site for meiotic gene conversion. Nature (London) **338:**87–90.
60. **Sun, H., D. Treco, and J. W. Szostak.** 1991. Extensive 3′-overhanging, single-stranded DNA associated with meiosis-specific double-strand breaks at the *ARG4* recombination initiation site. Cell **64:**1155–1161.
61. **Symington, L. S., and T. Petes.** 1988. Expansions and contractions of the genetic map relative to the physical map of yeast chromosome III. Mol. Cell. Biol. **8:**595–604.
62. **Szostak, J. W., T. L. Orr-Weaver, R. J. Rothstein, and F. W. Stahl.** 1983. The double-strand break repair model for recombination. Cell **33:**25–35.
63. **Thaler, D. S., and F. W. Stahl.** 1988. DNA double-chain breaks in recombination of phage λ and of yeast. Annu. Rev. Genet. **22:**169–197.
64. **Weiffenbach, B., D. T. Rogers, J. E. Haber, and M. Zoller.** 1983. Deletions and single base pair changes in the yeast mating type locus that prevent homothallic mating type conversions. Proc. Natl. Acad. Sci. USA **80:**3401–3405.
65. **Whelden, J. F., L. Gunn, and J. Nickoloff.** Unpublished data.
66. **White, C. I., and J. E. Haber.** 1990. Intermediates of recombination during mating type switching in *Saccharomyces cerevisiae*. EMBO J. **9:**663–673.
67. **Willis, K. K., and H. L. Klein.** 1987. Intrachromosomal recombination in *Saccharomyces cerevisiae*: reciprocal exchange in an inverted repeat and associated gene conversion. Genetics **117:**633–643.